Coupled ion and network dynamics in polymer electrolytes: Monte Carlo study of a lattice model

O. Dürr and W. Dieterich
Fachbereich Physik, Universität Konstanz, D-78457 Konstanz, Germany

A. Nitzan
Department of Chemistry, Tel Aviv University, Tel Aviv 69978, Israel

(Received 21 April 2004; accepted 5 October 2004)

Monte Carlo simulations are used to study ion and polymer chain dynamic properties in a simplified lattice model with only one species of mobile ions. The ions interact attractively with specific beads in the host chains, while polymer beads repel each other. Cross linking of chains by the ions reduces chain mobilities which in turn suppresses ionic diffusion. Diffusion constants for ions and chains as a function of temperature follow the Vogel–Tammann–Fulcher (VTF) law with a common VTF temperature at low ion concentration, but both decouple at higher concentrations, in agreement with experimental observations. Our model allows us to introduce pressure as an independent variable through calculations of the equation of state using the quasichemical approximation, and to detect an exponential pressure dependence of the ionic diffusion. © *2004 American Institute of Physics.* [DOI: 10.1063/1.1825371]

I. INTRODUCTION

Polymers carrying electronegative atoms (oxygen or nitrogen) in their repeat unit can act as solvents for certain salts, as a consequence of the attractive interaction between cations and the polymer. A prototype class of such polymer electrolytes are polyethers, e.g., poly(ethylene-oxid) (PEO), complexed with Li salts that contain a highly polarizable anion.[1–3] Above their glass transition temperature, in a supercooled fluid state, these materials can show significant ionic conductivities offering applications as electrolyte material in rechargable lithium-polymer batteries. In order to optimize electrochemical, mechanical, and thermal properties, materials with increasing complexity are being developed. These include alkali ionomers, where anions are chemically grafted to the polymer,[4] composites, where nanosize inorganic particles are added to the polymer-salt system,[5,6] gel electroytes,[7] as well as mechanically stretched chain electrolytes where experiments suggest that orientation of chains facilities ionic transport.[8,9]

At the same time, fundamental studies mostly on PEO-based electrolytes are pursued with the aim to elucidate the mechanism of cation transport, controlled by the local structure and dynamics of the host network. Indeed, ion and network mobilities are intimately connected: the ion migration depends on motions of polymer chain segments as evidenced by the decrease of cation mobilities on approaching the glass transition temperature T_g. On the other hand, it is known, e.g., for PEO-salt complexes that cations build a rather well-defined first coordination shell of oxygen atoms and hence form transient cross links within one chain or between different chains. Adding salt, the network stiffens and becomes more viscous as reflected by an increase in T_g.[10,11] Several molecular-dynamics (MD) studies provide direct evidence of cross link formation through cations.[12–14]

To investigate the interplay between ion and host matrix dynamics including slow diffusion and relaxation processes at temperatures in the vicinity of T_g, semimicroscopic models tractable by kinetic Monte Carlo (MC) simulation seem to be most promising.[15,16] Such models are not limited by the maximum time scales (of the order of nanoseconds) in present-day MD computations, which usually are too short to reach the regime of macroscopic diffusion. On the other hand, the main limitation of MC-simulations is the lack of a realistic microscopic description of chain conformation and ion coordination. Such properties certainly will enter the short-time dynamics, but are expected to play only a minor role at long times which we consider here. Thus we will rely on a coarse-grained lattice model for ions and polymer chains, where short-time and short–ranged processes are treated in a highly simplified manner. However, as we shall show, it provides a unique frame allowing us to reproduce important experimental trends in the long-time ion and chain dynamics as a function of temperature, pressure, and salt concentration. Experimental studies under varying salt concentration generally are carried out under constant pressure. As opposed to equilibrium simulations, efficient kinetic MC algorithms for lattice simulations at constant pressure are lacking.[17] Yet, introducing pressure as an independent variable and presenting transport properties under constant pressure is one of the goals of the present work that goes beyond earlier studies.[18] To accomplish this goal we resort to Guggenheim's quasichemical approximation (QCA) (Ref. 19) to obtain the equation of state (EOS), which is then combined with constant volume kinetic MC-simulations. The reliability of the QCA in a lattice model of a polymer host and solute particles was tested in previous investigations of ion solvation and dissociation equilibria.[20] As to the EOS, additional tests against simulations are discussed in Ref. 21.

The outline of the paper is as follows. After introducing our model and the simulation procedure (Sec. II) we derive

in Sec. III the equation of state by using the QCA. Section IV describes ion and chain diffusion properties at constant pressure for varying temperature and salt content, and the results are related to QCA configurational entropies in Appendix B. Pressure effects are discussed in Sec. VI, which also contains an analysis of how to combine empirical forms of a VTF-type temperature-dependence and an exponential pressure dependence of ionic diffusion constants.

II. LATTICE MODEL OF POLYMER ELECTROLYTES, SIMULATION TECHNIQUE

The mixture of polymers and ions is represented, respectively, by a system of lattice chains and pointlike particles on a simple cubic lattice with unit spacing. Beads of a chain molecule occupy a sequence of nearest-neighbor sites on the lattice. A site can either be vacant or singly occupied by an ion or a bead of a chain, implying a hard core repulsion among all beads and ions. In addition we assume a common nearest-neighbor repulsion $\epsilon>0$ among all beads. In view of the chain connectivity this introduces frustration and hence favors a transition from the fluid to an amorphous state.

With respect to their interaction with ions we distinguish two types of beads, X beads and C beads in PEO-type chain sequences $\mathrm{C}(X\mathrm{CC})_n$ where X corresponds to an oxygen atom. The length of chains is $r=3n+1$. Only relatively short chains will be considered such that entanglement effects will play no role. Since we are interested only in cation diffusion and in effects due to their specific interaction with chains, we take into account only one species of ions (cations) which attract nearest-neighbor X beads with a strength $-\epsilon_0>0$. Ions and C beads do not interact apart from site exclusion. Because our main interest is in systems with fairly small ion concentrations, we ignore ion-ion repulsions apart from site exclusion. In order to reduce the number of free parameters, we shall deal with only one energy scale and take $\epsilon=|\epsilon_0|$ throughout.

Originally, a model of this type has been proposed before in the description of solvation and ion pair dissociation in polymer electrolytes.[20] An extended version including Coulomb interactions between cations and anions has recently been investigated with respect to the specific differences in the diffusion properties of both ionic species.[15] The present restriction to only one species of mobile ions should be sufficient for the purpose of qualitatively discussing the profound effect of cross linking on cation diffusion and network rigidity, as attempted here. That restricted model also facilitates the QCA calculations in Sec. III and hence the conversion of results for diffusion at constant volume to the corresponding results at constant pressure. In this context one should mention certain polymer electrolytes, the so called ionenes where only cations are free to move while anions are chemically grafted to the polymer backbone.

To cope with the problem of generating thermalized configurations in a dense system, we use the configurational bias Monte Carlo algorithm by Frenkel[22] and Siepmann.[23] One Monte Carlo step consists in the removal and regrowth of part of a chain. The *a priori* weigth of an attempted MC step depends on factors which count the number of available bonds consistent with the hard core self-avoidance condition in each elementary growth step.[24] In turn, a new chain configuration is accepted according to the Metropolis rule. By contrast, the temporal evolution after equilibration is simulated using the generalized Verdier–Stockmayer algorithm[25,26] that involves kink-jump, end-jump, and crankshaft moves as elementary steps for polymer chains. Ions simply move via nearest-neighbor hops. Such ''physical'' moves have equal *a priori* probability and their acceptance probabilities are again chosen according to the Metropolis algorithm. At this point we remark that MC simulations of pure polymer melts are mostly carried out within the bond-fluctuation model.[27] However, for our system where ions are interacting with chemically heterogeneous chains the approach described above appears to be more natural.

Finally we briefly comment on lattice MC simulations of equilibrium properties under given pressure,[28] to be used in tests of the QCA of Sec. III. There we follow the method by Mackie *et al.*,[29] where volume fluctuations are induced by removing and adding lattice planes. Polymer chains which, for example, are cut upon removal of a lattice plane, are regrown with the help of the configurational bias method described above. For details we refer to the original literature.

III. QUASICHEMICAL APPROXIMATION

Guggenheim[19] has formulated a quasichemical approximation at the level of pairs for a general $(p+1)$-compound mixture that contains N_α chainlike molecules of species α $(\alpha=1,\ldots,p)$ with length r_α. The component $\alpha=0$ corresponds to the system of vacancies with $r_0=1$, while $\alpha=1$ is taken to refer to the system of ions, again with $r_1=1$. If the remaining molecules with $r_\alpha>1$ were homogeneous, the QCA equations determining the numbers $N_{\alpha\beta}$ of nearest-neighbor pairs (α,β) are

$$4N_{\alpha\alpha}N_{\beta\beta}=N_{\alpha\beta}^2\exp(\Delta\epsilon_{\alpha\beta}/k_BT) \tag{1}$$

with $\Delta\epsilon_{\alpha\beta}=\epsilon_{\alpha\alpha}+\epsilon_{\beta\beta}-2\epsilon_{\alpha\beta}$. As described in Sec. II, the interaction energies $\epsilon_{\alpha\beta}$ satisfy $\epsilon_{0\alpha}=0$ and $\epsilon_{11}=0$. Following Barker,[30] Eq. (1) remains valid when the two sets of X beads and C beads on our heterogeneous chains are treated as two kinds of molecules labeled by $\alpha=2$ and $\alpha=3$, respectively, with $N_2=N_3=N_P$ which is the number of polymer chains. By this, we have $\epsilon_{12}=-\epsilon_0$, $\epsilon_{13}=0$, and $\epsilon_{\alpha\beta}=\epsilon$ otherwise. The total number of bonds connected to molecules of type α is given by

$$2N_{\alpha\alpha}+\sum_{\beta\neq\alpha}N_{\alpha\beta}=zq_\alpha N_\alpha, \tag{2}$$

where z is the coordination number of the lattice and zq_α the number of unlinked nearest neighbor sites seen from all beads in a molecule of type α. Thus, for our system with chains of type $\mathrm{C}(X\mathrm{CC})_n$ we have $q_0=q_1=1$ and $zq_2=n(z-2)$ since X beads are always inner beads. Finally, $zq_3+zq_2=r(z-2)+2$ which is the total number of unlinked nearest-neighbor sites of a chain of length $r=3n+1$. With these relations the quantities $N_{\alpha\beta}$ in our model are determined by Eqs. (1) and (2). In order to get access to the thermodynamic potential $\Omega=\Sigma\epsilon_{\alpha\beta}N_{\alpha\beta}-TS_c$ we again fol-

low Barker[30] who gave an expression for the configurational entropy $S_c = k_B \ln g$, constructed such that the condition of a maximum with respect to $N_{\alpha\beta}$, subject to the restrictions imposed by Eq. (2), becomes identical to the quasichemical condition (1). The final result is

$$\ln g = \ln g_0 + \sum_{\alpha \leqslant \beta} \ln(N^*_{\alpha\beta}!/N_{\alpha\beta}!) + (\ln 2) \sum_{\alpha<\beta} (N_{\alpha\beta} - N^*_{\alpha\beta}), \tag{3}$$

where $N^*_{\alpha\beta}$ denotes the infinite temperature limit of $N_{\alpha\beta}$ and g_0 the number of configurations in the absence of interactions. In our model, g_0 is given by[19]

$$g_0 = \left[\left(\sum q_k N_k\right)!\right]^{z/2} \left[\left(\sum r_k N_k\right)!\right]^{1-z/2} (\Pi N_k!)^{-1} \rho N_P, \tag{4}$$

where the index k distinguishes vacancies, ions, and polymer chains. For the latter ($k=P$), we have $r_P = r$ and $q_P = q_2 + q_3$. The quantity ρ is the number of configurations of chains with one end fixed. Since chains in our model are relatively short, we can obtain ρ directly from exact enumeration of self-avoiding walks[31] or, approximately, from the assumption of Gaussian chains. Thereby it turns out that this last factor in Eq. (4) gives only a small (constant) contribution to $\ln g$.[32]

Minimization of Ω with respect to N_{00} and combination with Eqs. (1) and (2) yields the equation of state in the standard QCA form, where the pressure p is determined by the density N_0 and correlations N_{00} of vacancies,

$$-\frac{pa^3}{k_B T} = \ln\left(\frac{N_0}{M}\right) + \frac{z}{2} \ln \frac{2N_{00}M}{zN_0^2}. \tag{5}$$

Here M denotes the total number of lattice sites. While the first term on the right-hand side in Eq. (5) determines the pressure of a noninteracting lattice gas, the last term describes the influence of interactions through N_{00}. For example, if attractive interactions were dominant, clustering of vacancies enhances N_{00} and hence reduces the pressure when the volume $V = Ma^3$ is fixed. Conversely, for repulsive interactions as in the present model, N_{00} will be reduced and the pressure gets enhanced.

This QCA scheme has been used before in the special case $N_1 = 1$ as a lattice theory of solvation of an individual ion in a dense system of polyethers.[20] Quantitative tests of the equation of state (5) with varying N_1 gave remarkable agreement with Monte Carlo simulations in a model,[21] where links between successive beads were allowed to coincide not only with nearest-neighbor bonds, but also with second and third neighbor bonds on the simple cubic lattice. This situation of augmented degrees of freedom of chain molecules formally corresponds to a coordination number $z = 26$ and facilitates simulating the pressure by the method of Mackie *et al.*[29] relative to the case $z = 6$.[21] For our present nearest-neighbor model isotherms for the average volume per monomer are represented in Fig. 1. Different ion concentrations are parametrized by the ratio between N_1 and the number of oxygen beads in the system, $x = N_1/nN_2$. Upon increasing

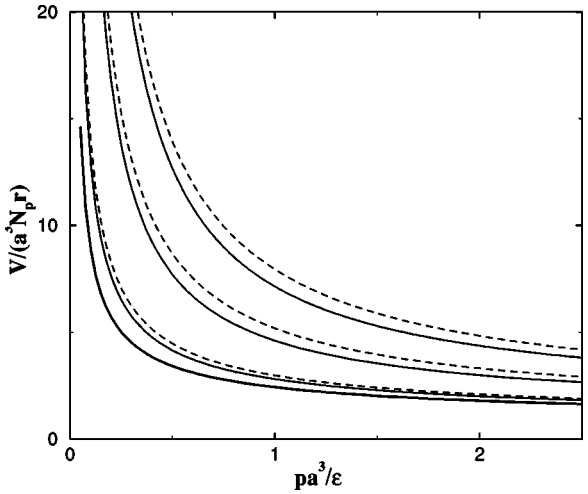

FIG. 1. Equation of state according to the QCA (full lines) for polymer chains of length $r = 10$ and ions with different concentration x. Plotted are isotherms belonging to $k_B T/\epsilon = 5$ and $x = 0$, 0.1, 1, and 2 (from below), representing the average volume per monomer in units of a^3 vs reduced pressure. Dashed curves represent the volume obtained when adding the partial volume of noninteracting pointlike particles with concentration x to the volume of the pure ($x = 0$) chain system.

x, the system swells less than one would expect by simply adding the partial volume $v_0 = a^3 N_1[1 - \exp(-pa^3/k_B T)]$ of noninteracting ions, see the dashed curves in Fig. 1. This obviously is a result of the attraction of ions by X beads. A test of the validity of the QCA scheme for $z = 6$ is shown in Fig. 2 for the number of ion-oxygen bonds N_{12}. Clearly, N_{12} increases as temperature drops. At temperatures $k_B T \lesssim \epsilon$, N_{12} becomes significantly larger than N_1. This means that each ion is bound on average to more than one X bead and therefore induces a cross link within or between chains. In that temperature range, when compared to simulations, N_{12} is overestimated somewhat by the QCA in the dilute case $x \ll 1$, whereas simulations and the QCA agree well for large x.

We add here a more detailed analysis of cross links in terms of the numbers $N_{1X}(n)$ of ions bound to n X beads, although these quantities are inaccessible by the QCA and are to be deduced from simulation. Obviously, $\Sigma_{n \geqslant 0} N_{1X}(n)/N_1 = 1$. From Fig. 3 we observe a monotonous decrease of $N_{1X}(0)$ as T decreases, while $N_{1X}(1)$ passes a maximum. By further lowering T, $N_{1X}(2)$ first increases at the expense of $N_{1X}(n)$ with $n < 2$. In Fig. 3(a) it then drops in favor of a growing $N_{1X}(3)$. For the concentrated system with more ions than X beads the behavior at high T is similar but data at low T indicate saturation of $N_{1X}(n)$ towards nonzero values.

Evidently we have

$$N_{12} = \sum_{n \geqslant 1} n N_{1X}(n). \tag{6}$$

At low T and small x, the first term $n = 1$ is negligible, as mentioned before. Obviously, the larger n, the more effective is the associated ion in restricting chain configurations. Hence, the remaining terms $n \geqslant 2$ in the weighted sum over

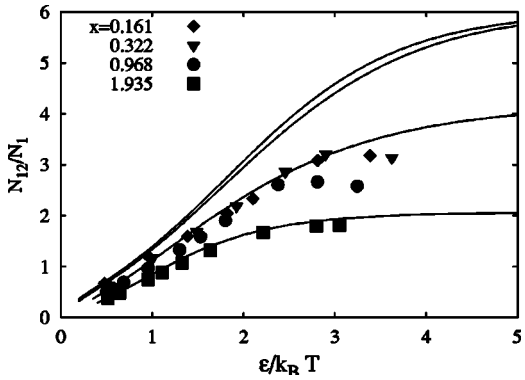

FIG. 2. Number of ion-oxygen bonds N_{12}, normalized by the number of ions N_1 vs inverse temperature for different x. Full lines: QCA. Data points: simulation.

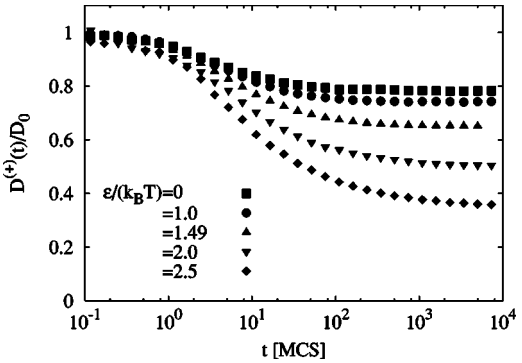

FIG. 4. Simulated time-dependent diffusion constant of ions $D^{(+)}(t)$ at a concentration $x=0.96$, normalized by the diffusion constant D_0 at infinite dilution, for different temperatures. The polymer host consists of $N_P=31$ chains in a volume $V=(10a)^3$.

$N_{1X}(n)$, Eq. (6), reflect the efficiency of ions to reduce chain entropies, an aspect to which we return in Appendix B.

IV. ION AND CHAIN DIFFUSION UNDER CONSTANT PRESSURE

Kinetic Monte Carlo algorithms allowing constant pressure simulations of lattice systems have been proposed in the literature but generally are not efficient enough to treat complex models as that defined in Sec. II. We therefore perform constant volume simulations but choose the volume $V=V(p,T)$ for given pressure p and temperature T according to the EOS derived in the preceding section. A nearly cubic simulation cell is chosen, with volume $a^3(L_1\times L_2\times L_3)=V(p,T)$, and periodic boundary conditions are applied in all three directions. In fact, for a given number of polymer beads and ions, values for p and T are taken such that L_1, L_2, and L_3 become integers which are close to each other. Typically we deal with $N_P=31$ chains of length $r=13$; hence an ion concentration $x=1$ corresponds to $N_1=124$ ions.

Clearly, this approach to pressure-dependent transport properties of a finite system will introduce some error because of the neglect of volume fluctuations for given p. An estimate of this error based on purely static considerations is provided in Appendix A. It turns out that this error is proportional to the inverse system size with a prefactor that gets enhanced near the glass transition.

Time-dependent mean-square displacements $\langle r^2(t)\rangle^{(k)}$ of ions $(k=+)$ and of the polymer center of mass $(k=P)$ allow us to deduce the corresponding long-time diffusion constants $D^{(k)}$ which are the quantities of primary interest. To illustrate the typical changeover from short-time to long-time diffusion, we have plotted in Fig. 4 the time-dependent diffusion constant of ions, $D^{(+)}(t)=\langle r^2(t)\rangle^{(+)}/6t$ at various temperatures. In contrast to diffusion in a medium with frozen disorder, realized, e.g., in glassy ionic conductors, dispersive transport effects are weak in the present model. (For example, $D^{(+)}(0)/D^{(+)}(\infty)\simeq 2.8$ at $\epsilon/k_BT=2.5$.) This is to be expected since local fluctuations in the polymer host provide a low-frequency cutoff to the spectrum of relaxation rates that determine $D^{(+)}(t)$.[33]

Figure 5 shows the T dependence of the long-time diffusion constants $D^{(+)}$ and $D^{(P)}$ at a reduced pressure $pa^3/\epsilon=0.35$ for various ratios x of the number of ions to X beads. In the Arrhenius representation of Fig. 5 the data points show a downward curvature and can well be represented by the Vogel-Tammann-Fulcher (VTF) law,[34–36]

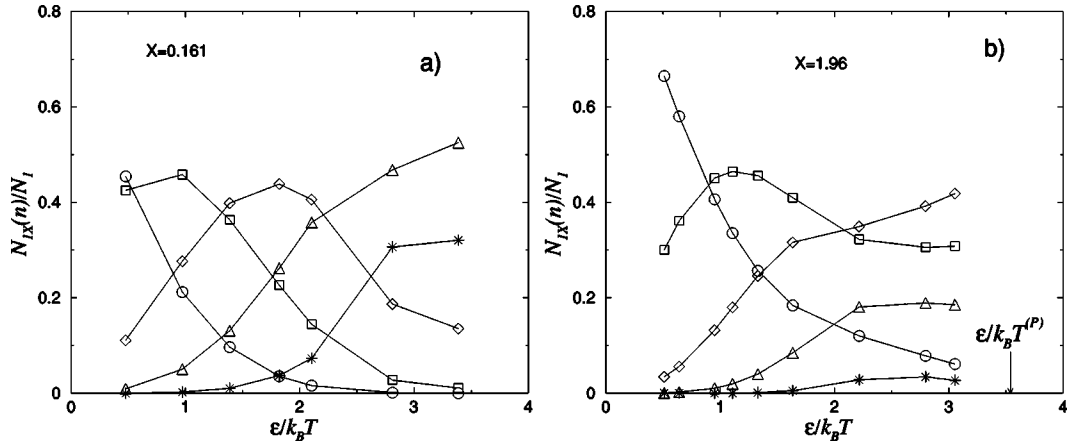

FIG. 3. Number of ions bound to n X beads, $N_{1X}(n)$, normalized by the total number of ions N_1 vs inverse temperature at $x=0.161$ (a) and $x=1.96$ (b).

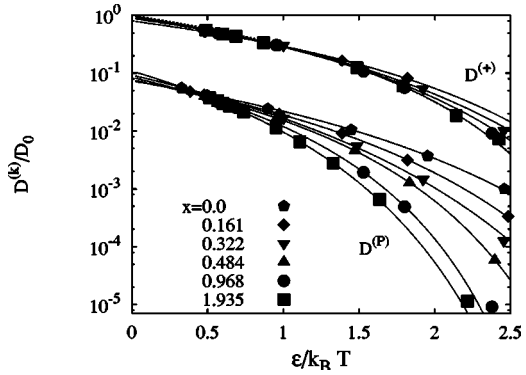

FIG. 5. Temperature-dependent diffusion constants for ions and polymer chains at various ionic concentrations x for fixed pressure $p=0.35\epsilon/a^3$. Full lines represent VTF fits, see Eq. (7).

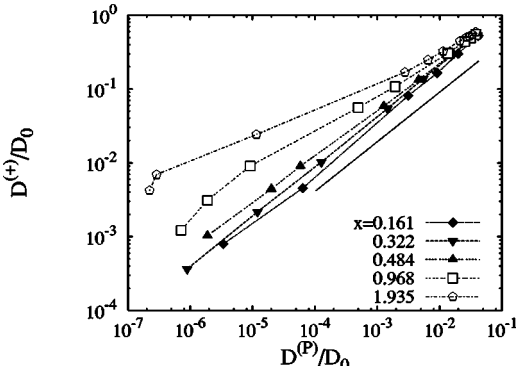

FIG. 7. Plot of ionic vs polymer diffusion constants after eliminating temperature, illustrating the validity of Eq. (8) for $x\lesssim 0.5$. The full straight line has a slope $\mu=0.67$.

$$D^{(k)}(T,x)=D_\infty^{(k)}\exp\left(-\frac{E^{(k)}(x)}{k_B[T-T^{(k)}(x)]}\right), \tag{7}$$

see the full lines in the figure. Note that the data in Fig. 5 covers a range of about four orders of magnitude in $D^{(P)}$. In Eq. (7) the prefactors $D_\infty^{(k)}$ denote the diffusion coefficients at infinite temperature, with $D_\infty^{(+)}=D_0$ the diffusion coefficient of free monomer particles and $D_\infty^{(P)}\simeq 10^{-1}D_0$ for the chain length considered. The quantity $E^{(k)}(x)$ is an energetic parameter and $T^{(k)}(x)$ the VTF temperature. One important observation is that both $D^{(+)}$ and $D^{(P)}$ are reduced when we increase the concentration of ions. This is to be expected from the assumption of our model, since ion binding to X beads induces cross links and hence will reduce chain mobilities. As a consequence, we observe that VTF temperatures $T^{(k)}(x)$ increase with x, as displayed in Fig. 6. The dashed line in the figure results from considerations of the configurational entropy, as explained in Appendix B. Generally, the VTF temperature represents a lower bound to the glass transition temperature T_g. Our simulations with respect to the diffusion of chains are therefore consistent with the experimentally observed increase in T_g with the ion content.[11,10] However, one has to be aware of the fact that experimentally the difference between both temperatures, $T_g-T^{(k)}$, may not remain constant during the variation of system parameters.[37]

Interestingly, for weakly doped polymers with $x\lesssim 0.5$ the VTF temperatures $T^{(P)}$ and $T^{(+)}$ roughly coincide, reflecting a strong coupling between ions and chains. As the number of ions becomes comparable to or larger than the number of X beads ($x\gtrsim 1$), ion and chain motions get decoupled, as can be seen from Fig. 6. Such a decoupling has been established experimentally for a variety of materials, for a review see Ref. 38. The corresponding VTF temperatures saturate for large x, with $T^{(+)}<T^{(P)}$, which means that for temperatures $T\sim T^{(P)}$ the ions maintain a certain mobility while the system of chains gets frozen.

Strong ion-chain correlations for small x can be analyzed from yet a different viewpoint. Keeping x fixed and eliminating temperature, we regard $D^{(+)}$ as a function of $D^{(P)}$. It turns out that for $x\lesssim 0.5$ the energy parameters $E^{(k)}(x)$ in Eq. (7) satisfy $E^{(+)}(x)\simeq\mu E^{(P)}(x)$ with $\mu\simeq 0.67$. Together with the fact that $T^{(+)}(x)\simeq T^{(P)}(x)$ for $x\lesssim 0.5$ this suggests that $D^{(+)}$ should vary with $D^{(P)}$ in a power-law fashion,

$$\frac{D^{(+)}}{D_\infty^{(+)}}\simeq\left(\frac{D^{(P)}}{D_\infty^{(P)}}\right)^{\mu}. \tag{8}$$

As seen from the double-logarithmic plot in Fig. 7, this relationship holds over almost four decades in $D^{(P)}$ and the slope displayed in cases $x\lesssim 0.5$ is indeed roughly independent of x. Qualitatively we expect that chain diffusion constants (for unentangled chains) reflect the viscosity η according to

$$\eta\propto(D^{(P)})^{-1}. \tag{9}$$

Combination with (8) expresses the ionic diffusion constant as a fractional power of the viscosity of the polymeric host, a relationship which can be regarded as a ''fractional Stokes-Einstein law.'' Such forms have been deduced before from measurements of the conductivity-viscosity relationship in ionic melts.[39,40] When $x\gtrsim 1$, ion and chain motions decouple, $T^{(P)}$ exceeds $T^{(+)}$ and Eq. (8) no longer holds. This is seen in Fig. 7, where data points for $D^{(+)}$ with $x\gtrsim 1$ fall above the low-concentration data sets with a slope μ.

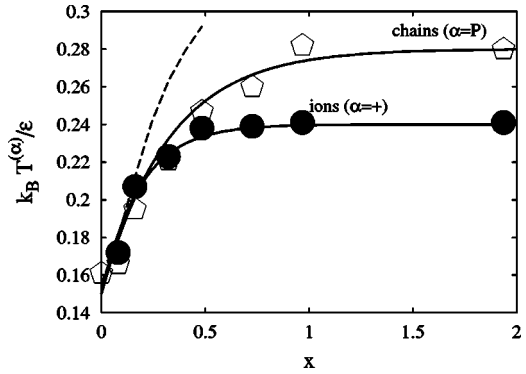

FIG. 6. VTF temperatures $T^{(+)}(x)$ and $T^{(P)}(x)$ for ions and chains as a function of ion concentration x (interpolated by full lines) at $p=0.35\epsilon/a^3$. The dashed line results from configurational entropy considerations, see the Appendix B.

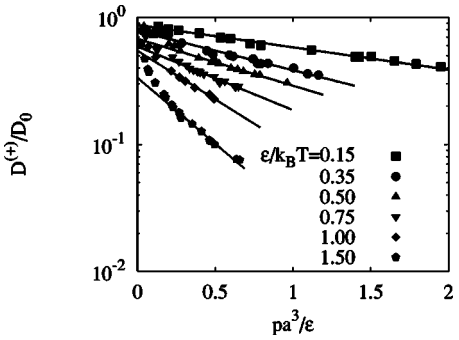

FIG. 8. Pressure dependence of ionic diffusion constants at different temperatures for $x=0.16$.

Finally, we briefly comment on the concentration dependence of the ionic conductivity $\sigma(x)$. When ion-ion correlations are neglected, $\sigma(x)$ becomes proportional to $xD^{(+)}(T,x)$. Experimentally, $\sigma(x)$ displays a maximum with respect to x.[10,11] One reason lies in the competition between an increasing charge carrier concentration x and network stiffening that causes a decrease in $D^{(+)}(T,x)$. It turns out that our data for $D^{(+)}$ in Fig. 5, which are limited to $\epsilon/k_BT<2.5$, do not show this feature after multiplication with x. For lower T, however, a more pronounced decrease of $D^{(+)}(T,x)$ with increasing x should be expected. A maximum in $\sigma(x)$ has been recovered in a recent model study of polymer electrolytes, based on Rouse chains with temporary cross links induced by the ions.[41]

V. PRESSURE-DEPENDENT IONIC DIFFUSION

As indicated before, we investigate the pressure dependence of $D^{(+)}$ in two steps: calculation of the volume for given pressure p with the aid of the EOS described in Sec. III, and N-V-T simulation of $D^{(+)}$ for that volume. Again we assume $N_P=31$ chains of length $r=13$ and take 20 ions so that $x=0.16$ is now kept constant. Figure 8 displays our results for various interaction constants ϵ/k_BT. Over the major part of the pressure range considered, $D^{(+)}$ displays the exponential behavior,

$$D^{(+)}(p,T)=D_0^{(+)}(T)e^{-p/p_0(T)}. \tag{10}$$

The slopes of the straight lines in the semilogarithmic plot in the figure reflect the quantity $p_0(T)$ which decreases with temperature. The steeper slopes towards small pressures $p \lesssim 0.1\epsilon/a^3$ must be regarded as an artifact of our model. In that range it shows an unrealistic volume expansion because of the lack of attractive interactions, so that the density falls below reasonable melt densities.

For pressures $p \gtrsim 0.1\epsilon/a^3$ our results can be compared with measurements of the pressure-dependent conductivity in polymer electrolytes[42,4] which indeed reflect an exponential p dependence, in agreement with Eq. (10). To relate the pressure scale in Fig. 8 to the physical pressure we note that the reduced pressure $pa^3/\epsilon=1$ corresponds to about 1 kbar which is the relevant experimental order of magnitude. This estimate is obtained by assuming a bond length $a \simeq 2$ Å and by noting that $k_BT^{(P)} \sim 0.2\epsilon$, see Fig. 6, which should be of the order of the experimental glass transition temperature $T_g \simeq 250$ K for polyethylene chains.

In view of the two empirical laws (7) and (10) the question arises how to represent $D^{(+)}$ in a consistent manner as a function of both variables T and p. This problem simplifies when we neglect the p dependence of $T^{(+)}$-data, which indeed vary by less than 10% and which seems to be justified also experimentally.[42] Equating the logarithms of Eqs. (7) and (10), both variables separate after differentiating with respect to p and T. It follows that $E^{(+)}=E_0+Ap$ and

$$[p_0(T)]^{-1}=\frac{A}{k_B(T-T^{(+)})}+B, \tag{11}$$

where the constants E_0, A, and B are fitted as $A \simeq 0.68a^3$, $B \simeq 0.69a^3/\epsilon$, and $E_0 \simeq 0.55\epsilon$. The prefactors in Eqs. (7) and (10) take the form

$$\begin{aligned} D_\infty^{(+)} &= \text{const}\exp(-Bp), \\ D_0^{(+)}(T) &= \text{const}\exp\left(-\frac{E_0}{k_B(T-T^{(+)})}\right). \end{aligned} \tag{12}$$

Equation (11) quantifies the decrease, noted earlier, of $p_0(T)$ with temperature. In our simulations of p-dependent diffusion we were limited to temperatures significantly larger than $T^{(+)}$, where both terms in Eq. (11) are of the same order. On the other hand, the analysis of experimental data in Ref. 4 for temperatures close to T_g amounts to setting $B=0$.

VI. SUMMARY AND OUTLOOK

Diffusion in a course-grained model of unentangled lattice chains and one species of pointlike particles (ions) subject to simplified chemical interactions has been studied by kinetic Monte Carlo simulations. Combination with the quasichemical approximation (QCA) for equilibrium properties allowed us to reproduce important trends in the ion and polymer host dynamics as a function of temperature, pressure, and ion content, which are observed in several PEO-type polymer electrolytes. Calculated diffusion constants show VTF behavior in their T dependence and an exponential p dependence. VTF temperatures, which increase with ion concentration due to cross linking of chains, were compared in Appendix B with DiMarzio's concept based on chain configurational entropies.

An important direction for future studies of ion transport through a polymer matrix is to develop an even more coarse-grained description, with the aim to retain only those polymer degrees of freedom which govern the elementary ionic migration steps, and to eliminate all others. A promising step in a system of athermal chains has been achieved recently in terms of dynamic percolation theory.[43,44] Relating models of interacting chains to dynamic percolation theory seems to be a challenging task.

ACKNOWLEDGMENTS

The authors would like to thank C. A. Angell, M. D. Ingram, P. Maass, and J. L. Souquet for interesting discussions. This work was supported in part by the Deutsche For-

schungsgemeinschaft (International Graduate College, "Soft Condensed Matter") and by the Kurt Lion foundation.

APPENDIX A

In this appendix we present an estimate of the difference between the "true" diffusion constant $D_{\text{true}}(p)$ at a given pressure p, including volume fluctuations, and the approximate quantity $D(p)=D_V(V(p))$ obtained in Sec. IV by neglecting volume fluctuations. Here $D_V(V)$ denotes the diffusion constant at fixed volume and $V(p)$ is determined by the EOS. In our notation for diffusion constants we suppress here the upper index $(+)$ and the other arguments besides p or V.

To introduce volume fluctuations we suppose that for a large but finite system sufficiently above T_g on can write $D_{\text{true}}(p)$ as an equilibrium average

$$D_{\text{true}}(p)=\int P(V|p)D_V(V)dV. \tag{A1}$$

The volume distribution function for fixed p, $P(V|p)$, is taken as a Gaussian with mean $V(p)$ and variance[45]

$$\langle(\Delta V)^2\rangle=-k_BT(\partial V/\partial p). \tag{A2}$$

Expansion of D_V up to second order with respect to $\Delta V=V-V(p)$ yields

$$D_{\text{true}}(p)-D(p)=\tfrac{1}{2}\langle(\Delta V)^2\rangle D_V''[V(p)]. \tag{A3}$$

Our discussion in Sec. V suggests expressing Eq. (A3) in terms of $D(p)$ and its derivatives, obtained from Eq. (10). This yields

$$\begin{aligned}[D_{\text{true}}(p)-D(p)]/D(p)&\\ =-(k_BT/2)[(\partial V/\partial p)(p_0(T)^2]^{-1}&\\ \times(1+p_0(T)(\partial^2V/\partial p^2)(\partial V/\partial p)^{-1}).&\end{aligned} \tag{A4}$$

Using results for the EOS in the relevant parameter range it turns out that the first term on the right-hand side of Eq. (A4) differs from the quantity $(rN_P)^{-1}(p_0(T)a^3/\epsilon)^{-2}$ only by a factor of order unity. The factor $(rN_P)^{-1}$ merely displays the expected proportionality to the inverse system size. As described before, in most of our calculations the system size was such that $rN_P=403$. For the lowest temperature considered in Fig. 8 it follows from Eq. (12) that $p_0(T)a^3/\epsilon \simeq 2.0$. Hence the first term in Eq. (A4) becomes of the order of 1%. A similar estimate holds for the second term in Eq. (16). However, lowering T and approaching the glass transition, $p_0(T)$ decreases as seen from Eq. (11). Equivalently, $D_V''(V)$ grows, showing that near the glass transition volume fluctuations in a finite system can become important for diffusion.

APPENDIX B

As shown previously, the QCA captures the main effects of cross linking and of the associated chain entropies on the dissociation-association equilibria of ions in polymer electrolytes.[20] This suggests that it should be possible to analyze the configurational entropy S_c of the present model, using Eq. (3) together with the solutions $N_{\alpha\beta}$ from Eq. (1).

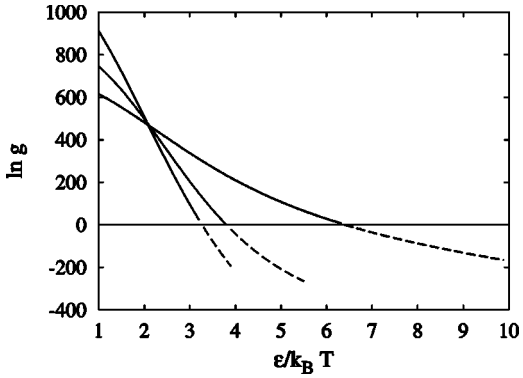

FIG. 9. Dimensionless configurational entropies $S_c/k_B=\ln g$ vs inverse temperature at a fixed pressure $p=0.35\epsilon/a^3$ calculated from the QCA. The three curves correspond to $x=0$, $x=0.323$, and $x=0.968$ in the order of intersection with the $\ln g=0$ line from right to left. Dashed parts of the curves are an artifact of the QCA.

At temperatures $k_BT\lesssim\epsilon$ and ion concentrations $x\ll 1$ we expect S_c to decrease upon increasing x, as a consequence of the formation of cross-linked chains. Among the quantities $N_{\alpha\beta}$ entering (3), the number of ion-oxygen bonds $N_{12}(x)$ will reflect the degree of cross linking, see also the discussion following Eq. (6), and will be most sensitive to variations in x.

Figure 9 shows the QCA configurational entropy $S_c(x,T)$ against the inverse temperature at a fixed reduced pressure $pa^3/\epsilon=0.35$. At $x=0$, the entropy reduction with decreasing temperature originates from repulsive bead-bead interactions. Introducing salt increases the entropy for high temperatures $k_BT/\epsilon\gtrsim 1$, since ion binding to oxygen beads becomes negligible, and free ions tend to expand the volume. As T is decreased, entropy curves drop more steeply than in the ion-free case, so that $S_c(x,T)$ falls below $S_c(0,T)$. Negative values for S_c are of course an artifact of the QCA, which generally should become less reliable when T is reduced. Nevertheless we can define a temperature $T_c(x)$ from the condition $S_c[x,T_c(x)]=0$ for the QCA entropy. Physically, $T_c(x)$ is supposed to merely indicate a characteristic temperature where the true configurational entropy becomes small in comparison with the value at ambient temperatures $k_BT\sim\epsilon$, so that configurations indeed get essentially frozen near $T_c(x)$. Interestingly, $T_c(x)$ defined in this way turns out to agree fairly well with the VTF temperatures $T^{(P)}(x)\simeq T^{(+)}(x)$ for small x. This is shown in Fig. (6) by the dashed line, which represents $k_BT_c(x)/\epsilon$, with $k_BT_c(0)/\epsilon\simeq 0.157$. These findings can be regarded as an illustration of DiMarzio's concept of a vanishing configurational entropy as a criterion for an ideal transition to an amorphous state.[46] From an experimental viewpoint that transition implies extrapolation to infinitely slow supercoolings, and the transition temperature is usually identified with the VTF temperature. In the present context this concept appears to describe the influence of cross linking of chain molecules on VTF temperatures in terms of the x-dependent configurational entropy. One should keep in mind, however, that the DiMarzio concept cannot be regarded to acquire general validity, as shown by accurate studies of the entropy in polymer models.[47] In addition, one should note that even the signifi-

cance of a VTF temperature is limited because its definition normally implies an extrapolation from considerably higher temperatures.

[1] F. M. Gray, *Polymer Electrolytes*, RSC Materials Monographs Vol. 1 (Royal Society of Chemistry, Cambridge, UK, 1997).
[2] M. Ratner and D. F. Shriver, Chem. Rev. (Washington, D.C.) **88**, 109 (1988).
[3] M. Ratner, *Polymer Electrolyte Reviews-1*, edited by J. R. McCallum and C. A. Vincent (Elsevier, New York, 1989), pp. 173–236.
[4] M. Duclot, F. Alloin, O. Brylev, J. Y. Sanchez, and J. L. Souquet, Solid State Ionics **136–137**, 1153 (2000).
[5] F. Croce, G. B. Appetecchi, L. Persi, and B. Scrosati, Nature (London) **394**, 456 (2001).
[6] M. Forsyth, D. R. MacFarlane, A. Best, J. Adebahr, P. Jacobsson, and A. J. Hill, Solid State Ionics **147**, 203 (2002).
[7] A. Reiche, R. Sandner, A. Weinkauf, B. Sandner, G. Fleischer, and F. J. Rittig, Polymer **41**, 3821 (2000).
[8] D. Golodnitzky and E. Peled, Electrochim. Acta **45**, 1431 (2000).
[9] O. Dürr, P. Maass, A. Nitzan, and W. Dieterich, J. Phys. Chem. B **106**, 6149 (2002).
[10] M. G. Mc Lin and C. A. Angell, Solid State Ionics **53–56**, 1027 (1992).
[11] S. Lascaud, M. Perrier, A. Vallée, S. Besner, J. Prud'homme, and M. Armand, Macromolecules **27**, 7469 (1994).
[12] B. Mos, P. Verkerk, S. Pouget, A. van Zon, G. J. Bel, S. W. de Leeuw, and C. D. Eisenbach, J. Chem. Phys. **113**, 4 (2000).
[13] J. J. de Jonge, A. van Zon, and S. W. de Leeuw, Solid State Ionics **147**, 349 (2002).
[14] F. Müller-Plathe and W. F. van Gunsteren, J. Chem. Phys. **103**, 4745 (1995).
[15] P. Pendzig, W. Dieterich, and A. Nitzan, J. Non-Cryst. Solids **235–237**, 748 (1998).
[16] J. F. Snyder, M. A. Ratner, and D. F. Shriver, J. Electrochem. Soc. **148**, A858 (2001).
[17] See, however, P. Pendzig, W. Dieterich, and A. Nitzan, J. Chem. Phys. **106**, 3703 (1997).
[18] Preliminary results were published in O. Dürr, P. Pendzig, W. Dieterich, and A. Nitzan, *Solid State Ionics: Science & Technology*, Proceedings of the Sixth Asian Conference on Solid State Ionics, Surajkund, India, December 1998, edited by B. V. R. Chowdari, and S. Chandra (World Scientific, Singapore, 1998), p. 33.
[19] E. A. Guggenheim, Proc. R. Soc. London **A183**, 203 (1944).
[20] R. Olender and A. Nitzan, J. Chem. Phys. **100**, 705 (1994); **101**, 2338 (1994); R. Olender, A. Nitzan, D. Knödler, and W. Dieterich, *ibid.* **103**, 6275 (1995).
[21] W. Dieterich, O. Dürr, P. Pendzig, and A. Nitzan, *Lecture Notes in Physics*, Proceedings of the 11th Max Born Symposium "Anomalous Diffusion: from Basics to Applications," Ladek Zdroj, Poland, May 1998, edited by R. Kutner, A. Pekalski, and K. Sznajd-Weron (Springer, Berlin, 1999), p. 175.
[22] D. Frenkel, G. Maoij, and B. Smit, J. Phys.: Condens. Matter **4**, 3053 (1992).
[23] J. Siepmann and D. Frenkel, Mol. Phys. **75**, 59 (1992).
[24] M. N. Rosenbluth and A. W. Rosenbluth, J. Chem. Phys. **23**, 356 (1955).
[25] P. H. Verdier and W. H. Stockmayer, J. Chem. Phys. **36**, 227 (1962).
[26] P. H. Verdier, J. Comput. Phys. **4**, 227 (1969).
[27] For a review see W. Paul and J. Baschnagel, in *Monte Carlo and Molecular Dynamics Simulations in Polymer Science*, edited by Kurt Binder (Oxford University Press, New York, 1995), Chap. 6, p. 307.
[28] O. Dürr, Diploma thesis, University of Konstanz, 1998.
[29] A. D. Mackie, A. Z. Panagiotopoulos, D. Frenkel, and S. K. Kumar, J. Chem. Phys. **102**, 1014 (1995).
[30] D. A. Barker, J. Chem. Phys. **20**, 1526 (1952).
[31] B. D. Hughes, *Random Walks and Random Environments* (Clarendon, Oxford, 1995), Vol. 1, Chap. 7.3.
[32] Using $r=13$, we have $\ln\rho\cong 18$, which at $x=0$ gives roughly an 8% contribution to $\ln g_0$.
[33] Significant conductivity dispersion in polymer electrolytes has recently been observed experimentally by V. Di Noto, M. Vittadello, S. Lavina, M. Fauri, and S. Biscazzo, J. Phys. Chem. B **105**, 4584 (2001); and by J. R. Dygas, B. Misztal-Faray, Z. Florjanczyk, F. Krok, M. Marzantowicz, and E. Zygadlo-Monikowska, Solid State Ionics **157**, 249 (2003). In this context it should be noted that motions of polar units in the polymer chains can contribute to the ac-conductivity, but this effect has not been explored in the present work.
[34] H. Vogel, Phys. Z. **22**, 645 (1921).
[35] G. Tammann and W. Hesse, Z. Anorg. Allg. Chem. **156**, 245 (1926).
[36] G. S. Fulcher, J. Am. Ceram. Soc. **8**, 339 (1925).
[37] H. V. Hubbard, J. P. Southall, J. M. Cruickshank, and G. R. Daviesand, I. M. Ward, Electrochim. Acta **43**, 1485 (1998).
[38] C. A. Angell, K. L. Ngai, G. B. McKenna, P. F. Mc Millan, and S. W. Martin, J. Appl. Phys. **88**, 3113 (2000).
[39] A. Voronel, E. Veliyulin, V. S. Machavariani, A. Kisliuk, and D. Quitmann, Phys. Rev. Lett. **80**, 2630 (1998).
[40] W. Dieterich, O. Dürr, P. Pendzig, A. Bunde, and A. Nitzan, Physica A **266**, 229 (1999).
[41] A. van Zon and S. W. de Leeuw, Electrochim. Acta **46**, 1539 (2001).
[42] J. J. Fontanella, M. C. Wintersgill, J. P. Calame, F. P. Pursel, D. R. Figueroa, and C. G. Andeen, Solid State Ionics **9–10**, 1139 (1983).
[43] O. Dürr, W. Dieterich, and A. Nitzan, Solid State Ionics **149**, 125 (2002).
[44] O. Dürr, T. Volz, W. Dieterich, and A. Nitzan, J. Chem. Phys. **117**, 441 (2002).
[45] L. D. Landau and E. M. Lifshitz, *Course of Theoretical Physics*, 3rd ed. (Butterworth-Heinemann, Oxford, 1980), Vol. 5, Chap. XII.
[46] E. A. DiMarzio, J. Res. Nat. Bur. Stand.-A. Phys. Chem. **68A**, 611 (1964).
[47] H. P. Wittmann, J. Chem. Phys. **95**, 8449 (1991).